# Computational Efficient Modeling of Sintering in Multi-component Alloys for ICME Applications

TESFAYE T. MOLLA, J.Z. LIU, and G.B. SCHAFFER

The major challenge while using sintering models for simulation of densification in multi-component alloys is finding the correct transport parameters, which are affected by not only temperature but also chemical composition and phase dispersion. A novel approach for determining the effective self-diffusivity and hence modeling the densification of engineering alloys during sintering is proposed. The approach integrates computational thermodynamics and simulation of diffusion-controlled transformations in multi-component alloys together with a low-order model for solid-state sintering. Computational thermodynamics, using the CALPHAD method, is used to predict microstructural phase stability, which is then used by diffusion simulation models to evaluate the effective transport properties for the sintering model. The modeling approach is validated by comparing results for densification of precipitation-hardened and austenitic stainless-steel alloys during an iso-rate sintering schedule with data from the literature. It is shown that the model can capture experimental observations very well. The modeling approach can thus be used in the development of an efficient search methodology for particulate materials within the context of an integrated computational materials engineering (ICME) frameworks.

https://doi.org/10.1007/s11663-019-01755-1


## I. INTRODUCTION

COMPUTATIONAL design of materials for efficient manufacturing requires simulating their behaviors during the processing cycle. Experimentally validated engineering models that are reliable, predictive and computationally efficient are thus crucial for the systematic design of alloys using, for instance, integrated computational materials engineering (ICME) techniques.[1,2] In the case of powder metallurgy (PM), complex numerical schemes are often used to simulate the evolution of structure descriptors, *e.g.*, density, during the sintering cycle.[3–6] However, integrating numerical models within an ICME framework can be computationally costly because material's design space is multi-dimensional and thus excessively large. For example, an alloy with ten components where the concentration of each component can take ten values may require billions of individual simulations during the exploration to identify the optimal alloy.[7]

Design frameworks that use low-order predictive models are one way to make the system tractable.[7] For design of alloys processed by PM, this requires low-order models that predict densification during sintering as a function of composition, temperature and time. Because the rate at which metal powders densify in the solid state is diffusion controlled, the major challenge in developing low-order sintering models for simulation of densification in multi-component alloys is finding the correct transport parameters (diffusivity) as a function of temperature and phase equilibria. We have previously developed an ICME framework for the design of particulate alloys consolidated by solid-state sintering.[8,9] However, those works did not contain a sintering model that could be used under different sintering profiles to validate the predictions against existing data.

Here we demonstrate an efficient and reliable approach for modeling the sintering response of engineering alloys that can be integrated within the existing ICME framework for the design of particulate materials. Initially, the method integrates computational thermodynamics with diffusion models to calculate the effective diffusivity in multi-component alloys. The effective diffusivities are then used in sintering models to estimate densification over time as well as temperature. The capability of the approach is demonstrated by comparing predictions of shrinkage strains in mono- and two-phase stainless-steel alloys with measurement

TESFAYE T. MOLLA, J.Z. LIU, and G.B. SCHAFFER are with the Department of Mechanical Engineering, The University of Melbourne, Parkville, VIC 3010, Australia. Contact e-mail: tesfaye.molla@unimelb.edu.au
Manuscript submitted June 12, 2019.
Article published online December 18, 2019.

data from the literature. The modeling approach is implemented in Matlab™ coupled with commercial thermodynamic and kinetic simulation tools, ThermoCalc (TC) and DICTRA, respectively.

## II. BACKGROUND TO THE SINTERING MODEL

Densification during solid-state sintering of a powder compact can be modeled by considering the modified version of the Nabarro-Herring creep equation.[10] The strain rate for linear shrinkage, $\dot{\varepsilon}_L$, during sintering is given by:

$$\dot{\varepsilon}_L = \frac{\dot{\rho}}{3\rho} = \frac{40}{3}\left(\frac{D_s\Omega}{G^2kT}\right)F_D \qquad [1]$$

where $\rho$ represents the relative density with $\dot{\rho} = \mathrm{d}\rho/\mathrm{d}t$; $D_s$ is the self-diffusion coefficient; $\Omega$ is the atomic volume; $G$ is the particle size; $k$ is the Boltzmann constant; $F_D$ is the driving force for sintering. In the case of free sintering (*i.e.*, sintering without any external load), the driving force for sintering is the intrinsic sintering stress, $\sigma_s$, and hence $F_D$in Eq. [1] can be replaced by the sintering stress. The sintering stress depends on the specific surface energy, $\gamma_s$, amount of porosity, $\theta$, and curvature of pores in the powder compact, and it is often given in the continuum theory of sintering as[11]:

$$\sigma_s = \frac{3}{2}\frac{\gamma_s}{G}(1-\theta)^2 \qquad [2]$$

By combining Eqs. [1] and [2], the linear shrinkage rate of the powder compact is given by:

$$\dot{\varepsilon}_L = 20\left(\frac{D_s\Omega\gamma_s}{G^3kT}\right)(1-\theta)^2 \qquad [3]$$

Considering conservation of mass, the volumetric shrinkage/strain rate, $\dot{\varepsilon}_v$, of a powder compact during sintering can also be expressed in terms of porosity, $\theta$, where, $\theta = 1-\rho$, as[11]:

$$\dot{\varepsilon}_v = 3\dot{\varepsilon}_L = \frac{\dot{\theta}}{1-\theta} \qquad [4]$$

Coarsening of particles during sintering can also be considered using an inverse square root function usually used for metallic powders involving a grain growth coefficient $k'$ and an initial particle size, $G_0$, as[12]:

$$G = \frac{k'G_0}{(1-\rho)^{1/2}} \qquad [5]$$

Here, $G$ represents the grain size of the primary phase (matrix). Note that in this study the suppression effect of the secondary phase (precipitate) on the grain growth of the matrix phase during the sintering cycle is assumed to be negligible.

In case of powder compacts involving engineering alloys, the self-diffusion coefficient in Eq. [3] needs to be replaced by the diffusion coefficient of the multi-component alloy, $D^{\text{eff}}$, which depends not only on temperature but also on the chemical composition of the alloy. Based on Onsager's formulation of Fick's law,[13] the one-dimensional effective diffusion coefficient of element-$i$, $D_i^{\text{eff}}$, in an alloy with $n$-components having a composition of $c$ is in general given by[14]:

$$D_i^{\text{eff}} = D_{ii}^n + \sum_j \frac{D_{ij}^n \partial c_j/\partial x}{\partial c_i/\partial x} \quad (i,j = 1,2,\ldots n \text{ and } i \neq j) \qquad [6]$$

In addition, in the case of alloys with multiple phase matrixes, it is necessary to solve Eq. [6] considering the phase distributions with the appropriate homogenization function.

Thus, to make use of the low-order predictive models of sintering for engineering purposes, it is critical to determine the effective diffusivity of engineering alloys during the entire sintering cycle not only as a function of temperature but also as a function of chemical and phase compositions. This makes the use of scarcely available mobility databases and analytical solutions quite difficult and requires numerical methods that can integrate phase-based calculations with those of diffusion-controlled transformation models and solve the complex differential equations efficiently.

## III. COMPUTATIONAL MODEL

The modeling approach involves (1) thermodynamic simulation based on the calculation of phase diagrams (CalPhaD), (2) simulation of diffusion in the multi-component alloy using the diffusion-controlled transformation (Dictra) model and (3) a reduced/low-order sintering model. Figure 1 shows the three components of the modeling approach together with summary of the information flow during simulation of sintering.

As discussed in Section II, the predictive capability of the low-order sintering model depends on the accuracy of the effective diffusively of the alloy, which is a function of the chemical composition and the phase stabilities at a given temperature, $T$. Thus, the sintering model is coupled with computational thermodynamics (CalPhaD) and a diffusional simulation model (DICTRA) to obtain an accurate estimation of diffusivity in the multi-component alloys.

### A. *Thermodynamic Simulation*

The thermodynamic simulation is performed using ThermoCalc (TC), a commercial software based on the calculation of the phase diagram (CalPhaD) method,[15] coupled with the appropriate thermodynamic databases. By considering the chemical composition of the alloy and temperature, TC is used to calculate the phase stability at a temperature, $T$, by minimizing the chemical potential or Gibbs free energy of the system. A single point equilibrium calculation for a given alloy with known compositions of alloying elements, temperature and pressure can be used to automate TC with other tools. The percentage by weight of each of the alloying elements together with the mole fraction of phases at the

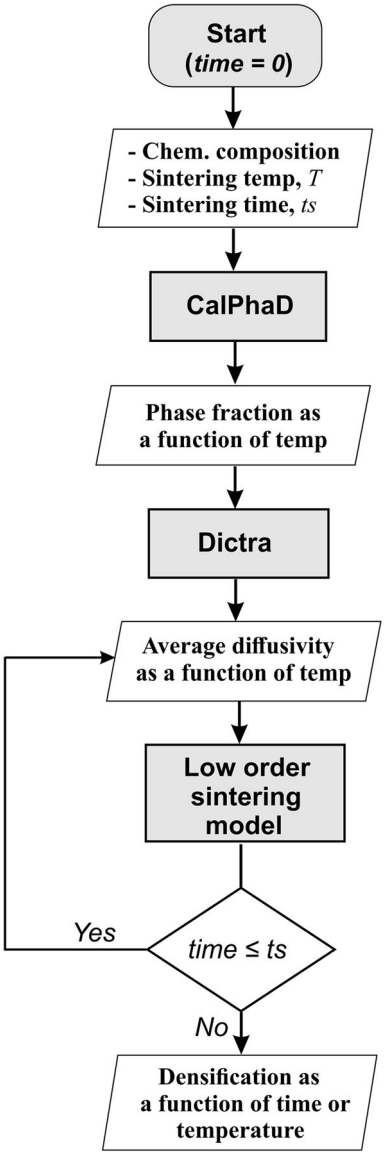


Fig. 1—Schematics showing flow of information in the proposed modeling approach.

temperature, $T$, are then used to set up a diffusion simulation model to estimate the effective diffusivity of the alloy.

## B. *Diffusion Simulation*

Determination of the effective transport parameters for a given alloy as a function of chemical composition and hence phase fractions can be performed by setting up diffusion simulation models. DICTRA is a flexible software for the simulation of diffusion-controlled transformations in multi-component alloys and has been used successfully to model a variety of alloy systems.[16] It requires coupling of thermodynamic (chemical potentials) and mobility databases.

The self-diffusion coefficient of an element in pre-alloyed powders can be estimated by simulating diffusion through a planar region consisting of the alloy's chemical composition and phase matrixes at the given temperature, as per the results from CalPhaD. To facilitate the simulation of the diffusion process, a closed system/region with mixed boundary condition (BC) involving flux of any of the element in the alloy can be used at one side. Simulation of diffusion through multiple phases requires defining an appropriate homogenization function to homogenize the effective transport property of an element in the alloy. Choice of the homogenization function depends on the required bound (lower/upper) of the effective property and microstructure of the alloy.[17]

The effective diffusivities as a function of temperature can thus be extracted using a number of isothermal diffusion simulation models at different temperatures along the sintering cycle. Note that the diffusion model provides the concentration profiles of alloying elements as a function of displacement, $x$, for a time, $t$. By considering the general solution for diffusion, see Eq. [7][10]; together with results of depth profiles (concentration *vs* distance), it is possible to calculate the effective diffusion coefficient of an element, $D_i^{\text{eff}}$, by plotting the argument of the complementary error function, $\arg\operatorname{erf}\left(c_{(x,t)} - c_o / c_f - c_o\right)$, against displacement, $x$:

$$c_{(x,t)} - c_o = \frac{c_f - c_o}{2}\left[1 + \operatorname{erf}\left(\frac{x}{2\sqrt{D_i^{\text{eff}} t}}\right)\right] \qquad [7]$$

where $c_o$ and $c_f$ are concentrations of the element under consideration at the boundaries with flux and closed BCs, respectively. Further details on this method can be found in Reference 10.

All three components of the model can be automated to exchange information as shown in Figure 1. The chemical composition and the sintering temperature-time profile can be considered as input parameters during modeling. CalPhaD is used to calculate the phase dispersion of the alloy along the sintering temperature profile. The initial input parameters together with outputs of the CalPhaD are then used in DICTRA to estimate the diffusivity of the major elements in the alloy. Note that successive DICTRA simulations are performed along the sintering temperature profile considering the corresponding phase composition. The average diffusivity of the alloy's powder compact is then calculated by considering the effective diffusion coefficients of all elements and their corresponding percentage by weight. Finally, the average diffusivity of the powder compact is used as an input to the sintering model to predict the linear shrinkage as well as densification of the alloy's green body during the sintering cycle.

Table I. Chemical Composition (Wt Pct) of the Alloys Used for Model Validation

| Powder | Fe | Cr | Ni | Cu | Mo | Mn | Nb | Si | C |
|---|---|---|---|---|---|---|---|---|---|
| 17-4PH | bal. | 16.7 | 4.9 | 4.6 | 0.17 | 0.63 | 0.3 | 0.60 | 0.04 |
| 316L | bal. | 17.2 | 11.2 | — | 2.6 | 1.8 | — | 0.76 | 0.03 |
| Aust-X | bal. | 15.3 | 7.6 | 2.2 | 2.64 | 0.31 | — | 0.96 | 0.06 |

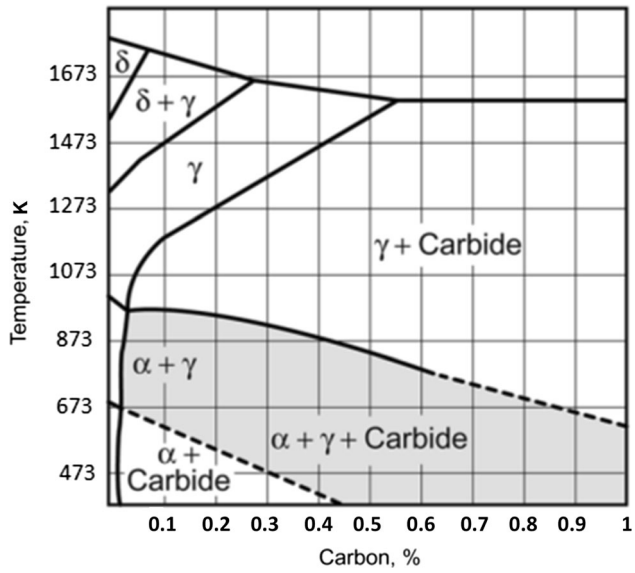


Fig. 2—Phase diagram of precipitation-hardened (17-4PH) stainless steel. Reprinted from Ref. [19].

## IV. VALIDATION OF MODEL

Experimental data of sintering for two stainless-steel alloys with mono- and two-phase dispersions are used to demonstrate the capability of the modeling approach. In a study to investigate the feasibility of co-sintering two metals, Imgrund *et al.*[18] reported densification measurements of an austenitic (316L) and a precipitation-hardened stainless steel (17-4PH) during an iso-rate sintering cycle. Both samples were sintered to 1300 °C with a constant heating rate of 5 K/min. The composition of the two standard alloys together with a new austenitic stainless-steel alloy (Aust-X) identified by Molla *et al.*[8] are shown in Table I.

For this discussion, we consider the sintering of 17-4PH stainless-steel powders. Injection-molded samples of 17-4PH powders are martensitic at lower temperatures or starting of sintering. During heating, however, the martensite structure in 17-4PH starts to transform to an austenitic structure. In addition, a second phase with ferrite structure will also start to form at higher sintering temperatures. These are shown by the phase diagram of 17-4PH in Figure 2.

Thus, it is evident that the sintering behavior in 17-4PH will be affected by the microstructural changes as a result of phase transformations during heating of the sample. Jung *et al.*[19] showed that the shrinkage rate in 17-4PH increases steadily from 1173 K to 1373 K resulting in the densification of the $\gamma$-austenite single phase. Between 1373 K and 1473 K, the shrinkage rate slope changes, indicating the appearance of a dual-phase microstructure involving $\delta$-ferrite and $\gamma$-austenite grains. The shrinkage rate increases once again above approximately 1478 K because of enhanced diffusion in a single $\delta$-ferrite phase. The experimental observation shows the importance of the effect of phase changes on the critical transport parameters used in the sintering models. Therefore, calculation of the diffusivity in the case of both 17-4PH as well as 316L powder compacts as a function of temperature needs to account for composition as well as phase changes and the proportions of each phase during heating.

Computational thermodynamics as well as diffusion-controlled transformation (Dictra) models are set up using the thermodynamic database for iron alloys, TCFE9, coupled with the mobility database, MOBFE4, to calculate the effective diffusion coefficients for the major alloying elements in the both alloys (*i.e.*, 17-4PH and 316L). Considering the compositions given in Table I, the thermodynamic and diffusion simulations are performed from 873 K to 1573 K at an interval of 100 K to extract the effective diffusion coefficients as a function of temperature. The effective diffusion coefficients are then used in the sintering model to estimate the shrinkage strains during the iso-rate sintering cycle to compare with the measurement data reported by Imgrund *et al.*[18]

Calculations of single point equilibrium at different temperatures across the heating profiles are coupled with diffusion simulation (Dictra) models. The Dictra models are used to simulate a 1D diffusion problem across a planar geometry with a width of 3 mm divided into 100 points (mesh nodes) distributed geometrically with a ratio of 1.03 to the side with flux BC to get more data points in the region where the concentration changes rapidly. It is assumed that the average diffusivity, $D^{\text{eff}}$, in the multi-component alloy depends primarily on the effective self-diffusivities of the major alloying elements (*e.g.*, Fe, Cr and Ni). The effective self-diffusivities of the major elements, $D_{\text{el}}^{\text{eff}}$ (where *el* represents one of the major alloying elements), are calculated after performing Dictra simulations with flux boundary conditions involving activity of each of the corresponding elements. Finally, the average diffusivity of the multicomponent alloy, $D_{\text{eff}}$, is found by considering the effective diffusivity of each of the major elements, $D_{\text{el}}^{\text{eff}}$, with their corresponding fraction of concentration, $f_{\text{el}}$, in the alloy as:

$$D^{\text{eff}} = D_{\text{Fe}}^{\text{eff}} f_{\text{Fe}} + D_{\text{Cr}}^{\text{eff}} f_{\text{Cr}} + D_{\text{Ni}}^{\text{eff}} f_{\text{Ni}} \quad [8]$$

Figure 3 shows a comparison between the average diffusion coefficients, $D_{\text{eff}}$, calculated by considering Fe, Cr, and Ni as the major elements in 17-4PH and 316L. The diffusion of the major alloying elements is

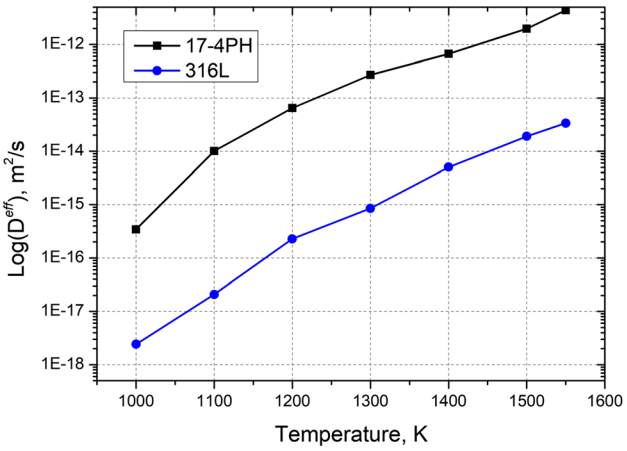


Fig. 3—The average diffusivities, $D^{eff}$, as a function of temperature in 17-4PH and 316L.

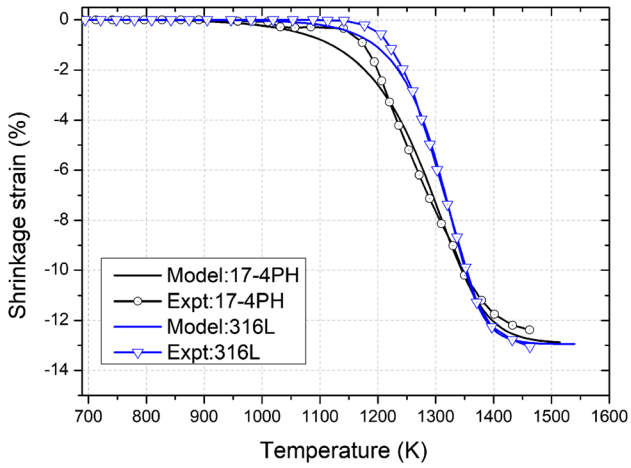


Fig. 4—Comparison of the model with experimental measurements of shrinkage strains during iso-rate sintering in 17-4PH and 316L.

**Table II. Parameters Used in the Sintering Model**

| | | |
|---|---|---|
| Heating Ramp, $T$ (K/min) | 5 | Ref. [18] |
| Atomic Volume, $\Omega$ ($m^3$) | $1.18 \times 10^{-29}$ | |
| Specific Surface Energy, $\gamma_s$ ($J/m^2$) | 2.60 | Ref. [8] |
| Boltzmann Constant, $k$ (J/K) | $1.38 \times 10^{-23}$ | |
| Grain Growth Coefficient, $k'$ (—) | 0.50 | Ref. [12] |

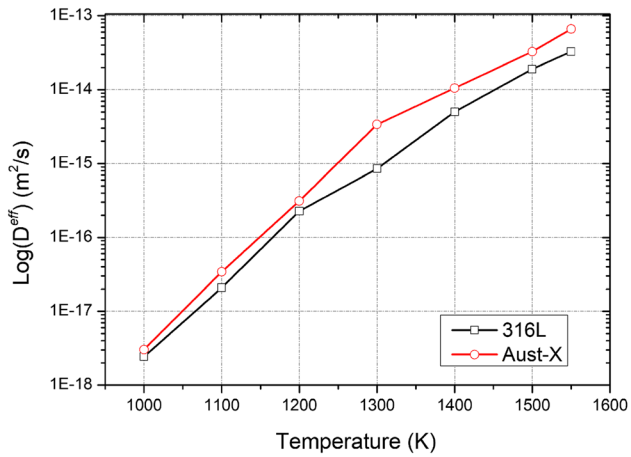


Fig. 5—Comparison of the average diffusion coefficients as a function of temperature between the proposed, Aust-X and 316L alloys.

significantly higher in 17-4PH than in 316L, implying a higher sintering activity in 17-4PH, as is observed experimentally.

The evolution of linear shrinkage strains in 17-4PH and 316L is predicted using the process parameters (green density, temperature, sintering cycle) given in Imgrund *et al.*[18] Since the initial particle sizes in Reference 18 are not uniform, the average value from the reported distribution of powder particles is used. Table II summarizes the other parameters used in the sintering model.

Figure 4 shows the comparison of model predictions with those of measurements for the evolution of the shrinkage strains during iso-rate sintering from 700 K to 1573 K. It is evident to see that 316L mainly densifies at higher temperatures compared with 17-4PH. In both alloys, the predictions agree well with the measurements showing the capability of the model despite the assumptions made on particle size.

## V. APPLICATION OF THE MODELING APPROACH

Designing multi-component alloys for performance properties coupled with processing characteristics often requires searching through vast composition space. Here, we show the importance of the model developed in this study to predict the sintering characteristics of alloys during the design of new materials. An example of a stainless-steel alloy with a composition shown in Table I, *i.e.*, Aust-X, which has been tested (using CalPhaD) to be austenitic at higher sintering temperatures, is considered. This alloy was identified after optimizing the chemical composition of austenitic stainless-steel alloy for sintering and solid-solution hardening at 1600 K using a low-order ICME design framework.[8] Here, this alloy is used to demonstrate the effect of compositions on the effective diffusion coefficients and hence densification characteristics of multi-component alloys by comparing with standard austenitic stainless-steel alloy, 316L.

As discussed in Section III, computational thermodynamics and diffusion transformation models coupled with thermodynamic and mobility databases for iron-based alloys are used to determine the effective diffusion coefficient for the Aust-X as a function of temperature. Figure 5 shows comparison of the diffusion coefficients for Aust-X and 316L, where higher diffusions are observed consistently at higher temperatures in Aust-X because of variations in chemical compositions only.

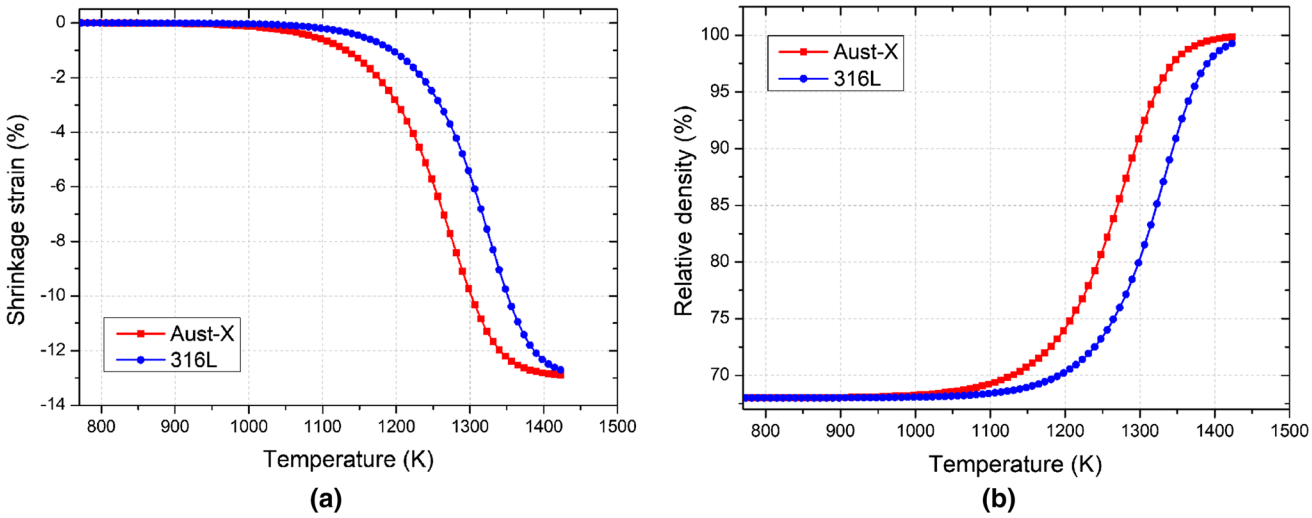


Fig. 6—Comparison of model prediction for (*a*) shrinkage strains and (*b*) relative density between the standard austenitic steel and new austenitic alloy after sintering for 2 h.

The addition of copper (Cu) in Fe-based alloys enhances the diffusivity of the austenite (FCC) Fe and hence increases the effective diffusivity of the overall powder compact of the alloy at higher temperatures. The effect of copper and other alloying elements on the diffusivity of austenitic stainless steels at the sintering temperatures were shown by Molla *et al.*[8] Thus, the effective diffusivity of the alloy can be used in the sintering model discussed in Section II to evaluate the densification of powder compacts in any types of sintering schedules.

For sake of demonstration, the evolution of linear shrinkage strains in Aust-X and 316L in a constant rate sintering schedule is predicted using the process parameters (green density, temperature, sintering cycle) discussed in Section IV. The initial particle sizes in both cases are assumed to be equal with values of 3.6 $\mu$m. The sintering is assumed to be performed for 2 hours at a constant rate of 5 K/min. Figure 6(a) shows the evolution of shrinkage strains as a function of temperature in both alloys.

The densification in Aust-X shows a significant improvement compared with densification of 316L. This can be further shown by the difference in the evolution of the relative density as a function of temperature; see Figure 6(b). For instance, at 1300 K the model predicts a 10 pct difference in the relative density between Aust-X and 316L, achieved by varying the composition of the alloy.

The model suggested here can also be combined with mechanical property models to predict, for instance, the strength of alloy powder compacts as a function of the final density using any kind of sintering schedules. This is useful for modeling the effect of process parameters such as heating rates as design variable during computational design of multi-component alloys processed by a sintering process.

## VI. CONCLUSION

A novel approach for determining the effective self-diffusivity and hence modeling the densification of engineering alloys during sintering is proposed. The model is developed to enable an efficient search for unique particulate materials within an integrated computational materials engineering (ICME) framework. The approach integrates a low-order model for solid-state sintering with computational thermodynamics and simulation of diffusion-controlled transformations in multi-component alloys. Thermodynamic calculations, using the CALPHAD method, are used to predict microstructural stability whereas simulations of diffusion in multi-component and/or multi-phase alloy systems are used to evaluate the effective transport parameters as a function of temperature, composition and phase dispersion. The modeling approach is validated by comparing results for densification of precipitation hardened and austenitic stainless-steel alloys during iso-rate sintering with data from the literature. It is shown that the model can accurately capture experimental observations. The model is also used to investigate the role of alloy composition for improving the sintering behavior of an austenitic stainless steel demonstrating its usefulness in the development of low-order ICME frameworks for designing powder processed engineering alloys.

## FUNDING

This work was funded by The University of Melbourne.

## COMPETING INTERESTS

The authors declare no competing interests.

## REFERENCES

1. G.B. Olson: *Science*, 1997, vol. 277, pp. 1237–42.
2. G.B. Olson: *Acta Mater.*, 2013, vol. 61, pp. 771–81.
3. F. Wakai and K. Brakke: *Acta Mater.*, 2011, vol. 59, pp. 5379–87.
4. G. Brown, R. Levine, V. Tikare, and E. Olevsky: *Adv. Sinter. Sci. Technol.*, 2010, vol. 209, pp. 103–11.
5. S. Nosewicz, J. Rojek, K. Wawrzyk, P. Kowalczyk, G. Maciejewski, and M. Maździarz: *Comput. Mater. Sci.*, 2019, vol. 156, pp. 385–95.
6. T.T. Molla, R. Bjørk, E. Olevsky, N. Pryds, and H.L. Frandsen: *Comput. Mater. Sci.*, 2014, vol. 88, pp. 28–36.
7. A. Deschamps, F. Tancret, I.E. Benrabah, F. De Geuser, and H.P. Van Landeghem: *Comptes Rendus Phys.*, 2018, vol. 19, pp. 737–54.
8. T.T. Molla, J.Z. Liu, and G.B. Schaffer: *Integr. Mater. Manuf. Innov.*, 2018, vol. 7, pp. 136–47.
9. T.T. Molla, J.Z. Liu, and G.B. Schaffer: *J. Integr. Mater. Manuf. Innov.*, 2019, vol. 8, pp. 82–94.
10. M.N. Rahaman: *Sintering of Ceramics*, Taylor and Francis Group, Boca Raton, FL, 2008.
11. E.A. Olevsky: *Mater. Sci. Eng. R*, 1998, vol. 23, pp. 41–100.
12. R.M. German: *Crit. Rev. Solid State Mater. Sci.*, 2010, vol. 35, pp. 263–305.
13. L. Onsager: *Ann. N. Y. Acad. Sci.*, 1945, vol. 46, pp. 241–65.
14. M.A. Dayananda: *Defect Diffus. Forum*, 1993, vols. 95–98, pp. 521–36.
15. M. Perrut: *J. AerospaceLab*, 2015, vol. 9, pp. 1–11.
16. A. Borgenstam, A. Engstro, L. Ho Lund, and J.A. Ren: 2000, vol. 21, pp. 269–80.
17. H. Larsson and A. Engström: *Acta Mater.*, 2006, vol. 54, pp. 2431–39.
18. P. Imgrund, A. Rota, F. Petzoldt, and A. Simchi: *Int. J. Adv. Manuf. Technol.*, 2007, vol. 33, pp. 176–86.
19. I.D. Jung, S. Ha, S.J. Park, D.C. Blaine, R. Bollina, and R.M. German: *Metall. Mater. Trans. A*, 2016, vol. 47A, pp. 5548–56.